CAMBRIDGE
UNIVERSITY PRESS

RESEARCH ARTICLE

Evaluating possible sources of error in tree-ring ^{14}C data using multiple trees across South America

Guaciara M Santos[1] , Lucas D Nguyen[1], June N Griffin[1], Nathan de Oliveira Barreto[2],
Daigard R Ortega-Rodriguez[2], Ana Carolina Barbosa[3] and Gabriel Assis-Pereira[2]

[1]Department of Earth System Science, University of California Irvine, Irvine, CA, USA, [2]Departamento de Ciências Florestais, Universidade de São Paulo, Piracicaba, Brazil and [3]Departamento de Ciências Florestais, Universidade Federal de Lavras, Lavras, Brazil

Corresponding author: Guaciara M Santos; Email: gdossant@uci.edu

Abstract

A limitation in fine-tuned tree-ring radiocarbon (^{14}C) data is normally associated with overall data uncertainty. Tree-ring ^{14}C data variance as a result of sample heterogeneity can be reduced by adopting best practices at the time of sample collection and subsequent preparation and analysis. Variance-reduction of ^{14}C data was achieved by meticulous sample handling during increment core or cross-sectional cuttings, in-laboratory wood reductions, and cellulose fiber homogenization of whole rings. To demonstrate the performance of those procedures to final ^{14}C results, we took advantage of the replicated data from assigned calendar years of two Pantropical post-1950 AD tree-ring ^{14}C reconstructions. Two *Cedrela fissilis* Vell. trees spaced 22.5 km apart, and two trees of this species together with one *Peltogyne paniculata* Benth tree spaced 0.2 to 5 km apart were sampled in a tropical dry and moist forest, respectively. Replicate ^{14}C data were then obtained from grouped tree-ring samples from each site. A total of 88% of the replicated ^{14}C results fell into a remarkably consistent precision/accuracy range of 0.3% or less, even though multiple tree species were used as pairs/sets. This finding illustrates how adopting a few simple strategies, in tandem with already established chemical extraction procedures and high-precision ^{14}C analysis, can improve ^{14}C data results of tropical trees.

1. Introduction

The tropics are the most biologically diverse and important areas in the world (Ter Steege et al. 2015), yet radiocarbon (^{14}C) measurements on tropical tree rings are relatively sparse. Recent advances in tropical dendrochronology have shown that several tropical trees can produce recognizable annual bands due to cambial dormancy, driven by annual seasonality in environmental conditions (Brienen et al. 2016). As wood cells develop and fix ^{14}CO$_2$ from the atmosphere during the growing season, tree rings can reflect the atmospheric ^{14}C signal at the time the tissue was formed. Provided that annually resolved tree rings have been found and were validated by measuring ^{14}C of selected calendar years after 1950 AD (which provides a high time resolution reference of ≤ 1 year—Fontana et al. 2024; Hadad et al. 2015; Haines et al. 2018; Pearson et al. 2011; Santos et al. 2020, 2021), they can be further used to address observation-based atmospheric ^{14}C records. This is relevant, due to the shortage of robust atmospheric ^{14}C records across the tropics (Santos et al. 2020).

Global atmospheric ^{14}C concentrations post-AD 1950 are typically divided into five geographical zones (Hua et al. 2022), e.g., three across the Northern Hemisphere (NH1, NH2, and NH3), and two over the Southern Hemisphere (SH1-2 and SH3). As part of a major effort to produce and integrate high quality annual tree-ring records of past atmospheric ^{14}C into future age calibration compilations

(Hua et al. 2022), researchers have produced novel ^{14}C records using dated tree rings from tropical and subtropical South America (Ancapichún et al. 2021; Santos et al. 2015, 2022, 2024). Still, the methodology is intrinsically challenging, as it demands costly and laborious work. For example, ^{14}C measurements using annual tree rings involve a sequence of i) sampling material from radial directions removed from cross-sections or increment cores in the field, ii) dating the trees and marking the selected tree rings for later wood subsampling, iii) careful isolation of tree rings with a scalpel, iv) chemical procedures to isolate inert carbon fractions (such as holocellulose and alpha-cellulose extracts), v) sample processing to CO_2 and/or filamentous graphite, and finally vi) analysis by specific analytical instruments (such as, accelerator mass spectrometry—AMS).

Each of those steps can introduce uncertainties to the final results. Santos et al. (2015) and Turnbull et al. (2017) reported differences in ^{14}C data replication and attributed them to the difficulty of separating tree rings at their boundaries. Svarva et al. (2019) went a step further, adding that inhomogeneities in the tree-ring cellulose extracts can also lead to differences in ^{14}C data replication.

In principle, ^{14}C data variance can be extremely high on single tree-ring analysis when wood material has been mistakenly added, or accidentally lost during the cutting up of wood sections for further ^{14}C analysis. Specifically, tree-ring subsampling from laths can experience both exclusion of portions of the desired growing season, or unintentional inclusion of more than one season. In the laboratory, caution is also required during single tree-ring reduction to particles (a maximum % yield recovery is desirable), and/or cellulose partitioning for the CO_2 combustion step before the ^{14}C-AMS measurements take place (use of homogenized fibers is advised). Radiocarbon variance among tree-ring replicated results tend to be higher during the increase of atmospheric ^{14}C levels after nuclear bomb tests in the early 1950s (Enting 1982), and its subsequent decline due to the 1963 moratorium on above ground testing (Levin and Hesshaimer, 2000). During those periods, the relative level of ^{14}C absorbed by wood material changes greatly from the onset to the end of wood cell formation. Thus, one should expect differences in ^{14}C signatures when the wood material analyzed is imprecisely subsampled relative to the distinct lines (ring boundaries or earlywood/latewood boundaries) that demarcate a single tree ring (Turnbull et al. 2017). The effect of accidentally losing wood material during the early stages of sample handling can mimic the ^{14}C results of selective earlywood or latewood measurements (e.g., Haines et al. 2023; Kudsk et al. 2018).

As instrumentation has advanced, especially AMS systems used in ^{14}C analysis (Bronk Ramsey 2023), analytical uncertainties have decreased to well under 0.3% (Sookdeo et al. 2020, for example). Further evaluations of sources of errors in tree-ring ^{14}C data are still required. Notably, it is difficult to separate cause and effect when so many steps are involved in tree-ring sample processing for isotopic analysis, as aforementioned. Overall, differences in chemical extractions and spectrometers may not be the only factors causing data variability. Several researchers have compared ^{14}C data from distinct chemical methods, e.g., holocellulose versus alpha-cellulose (Baker et al. 2017; Capano et al. 2018; Cercatillo et al. 2021; Michczyńska et al. 2018; Němec et al. 2010; Santos et al. 2023; Southon and Magana 2010), independent chemical treatments of alpha-cellulose (Gaudinski et al. 2005; Santos et al. 2024), extractions using different apparatus or devices (Fogtmann-Schulz et al. 2021; Santos et al. 2020; Southon and Magana 2010), as well as different types of mass spectrometers of laboratory analysis (Baker et al. 2017; Kudsk et al. 2021; Santos et al. 2022, 2024; Sookdeo et al. 2020). Regardless of differences in approach, ^{14}C results have been somewhat similar within uncertainties ($\pm$ 2σ). For example, holocellulose versus alpha-cellulose extractions of Holocene samples among distinct laboratories yielded pooled standard deviations of 0.25% or lower (n = 5 pairs/sets) (Santos et al. 2023); alpha-cellulose extractions from independent chemical procedures and apparatus yielded standard deviations of 0.3% (n = 27 pairs/sets; Santos et al. 2022); and different ^{14}C-AMS facilities' alpha-cellulose procedures and ^{14}C analysis yielded standard deviations of 0.17% (n = 10 pairs/sets; Santos et al. 2024). Here, pooled standard deviation values were calculated using the formulation shown in Cohen (1988), as a way to assess data quality.

In order to separate spatial and temporal heterogeneity in the tree-ring samples, from chemical and/or analytical uncertainties, Santos et al. (2023) focused on evaluating the very early stages of wood sample

handling as well as cellulose extract homogeneity. Depending on its growth triggers and sites (Baker et al. 2017), different tree species may experience different growing season lengths. Therefore, Santos et al. (2023) emphasize the inclusion of earlywood and latewood from each full tree-ring sample analyzed. This can be done through the microscope inspection of tree-ring samples before samples are reduced to small particles (e.g., wood chips or slivers) for chemical processing. Variance-reduction strategies, as reported in Santos et al. (2023), have then been used in the production of two post-AD 1950 atmospheric ^{14}C records across the Amazon when using single absolutely dated trees (e.g., tree-ring ^{14}C records produced from Central and Eastern Amazon Basin) (Santos et al. 2022 and 2024, respectively). Nonetheless, just one dendrochronologically-dated tree was used per site studied.

The goal of this work is threefold: i) to reevaluate the aforementioned variance-reduction strategies in multiple tree species; ii) test data consistency among several trees on a given site (same species or different species); and iii) evaluate data consistency among trees based on their distances apart on a given site. For all of those, we present ^{14}C tree-ring data of two post-AD 1950 Pantropical sites and their coexisting trees (same or distinct species). Those sites and samples pertain to a project to complete post-1950 ^{14}C records with the goal of mitigating important deficiencies of the current ^{14}C atmospheric global map over the Tropical Low-Pressure Belt (TLPB; conventionally termed the Inter-Tropical Convergence Zone). Those records are timely (Reimer et al. 2020), given the dearth of datasets that can elucidate air transportation and climatic variability affecting atmospheric ^{14}C concentrations across this region. Thus here, we took advantage of the ^{14}C pairs/sets produced from the tree-ring calendar years associated with the post-1950 slopes, i.e., periods of major atmospheric ^{14}C signature changes where small offsets can be highly detectable, to identify methods to improve precision and accuracy. These points are paramount for the assessment of the likely impact of our soon-to-be published Pantropical ^{14}C records. As such, climatic patterns and geographic provenance of air-masses to sites are not pursued in depth in the present article, as they are not in the scope of this work. As already mentioned, to evaluate the reproducibility of the ^{14}C data, we made use of the pair/sets of the overlapping calendar years, i.e., replicated data from each atmospheric ^{14}C record at a given location. For accuracy data discussions, we use the current atmospheric zonal $^{14}CO_2$ curves (such as SH1-2 and SH3, as defined in Hua et al. 2022), when using multiple tropical trees at single locations.

2. Materials and methods

2.1 Sites and samples

The ^{14}C data discussed in this work are from samples collected at two localities in South America. Vegetation growth in South America is strongly regulated by the South American Monsoon System (SAMS), occurring between September and May (Novello et al. 2017). Ring growth, however, follows more specific site climatic conditions (e.g., the Köppen climate classification of each specific region – Figure S1). Thus, our comparisons explored i) tropical dry and moist forest conditions (Figure 1); ii) more than one tree and/or species per site, where trees were collected from dead (cross-section) and/or live (increment-core) individuals; and iii) source areas, as trees were separated by a range between 0.2 and 22.5 km (Figure 2).

Trees from the Rio São Francisco Basin, specifically those from Juvenília, Minas Gerais, Brazil (blue star in Figure 1A) experience a long dry season followed by a wet season of heavy rainfall. Since Cedrela species' tree growth and reproduction are normally synchronous with the onset of the rains, we used a climate classification diagram to determine the period of tree growth across this region (November to March; Figure S1).

Trees at the Juvenília site consisted of dendrochronologically correlated *Cedrela fissilis* trees (Pereira et al. 2018). The series MTV001D and MTV114B (Figure 2), originating from MTV001 (1882 to 2015) and MTV114 (1994 to 2015) trees, respectively, were selected for ^{14}C dating. In the first tree, ring widths were measured on four radii (cross section), while in the second, ring widths were measured on two radii (cores). The intercorrelation between the two series was r=0.692 (Table S1). Even so,
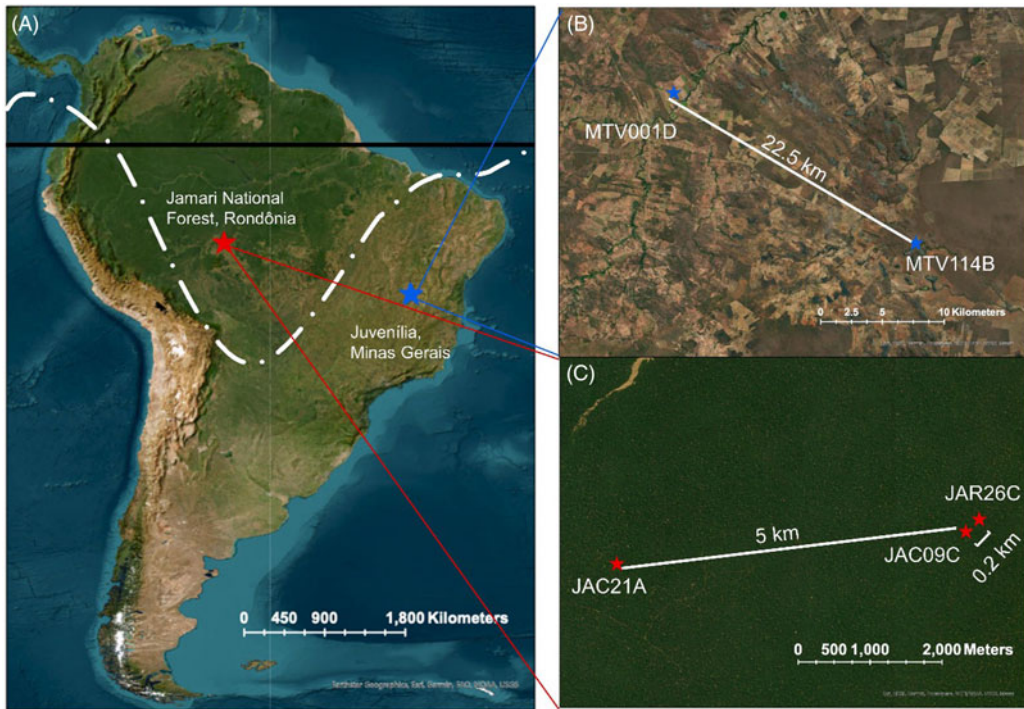
Figure 1. *Map of South America, detailing the two sample sites in Brazil (A), i.e., Juvenília, Minas Gerais (blue star) and Jamari National Forest, Rondônia (red star). Aerial view of the Juvenília site, and tree locations for the* Cedrela fissilis *samples, MTV001D (cross-section) and MTV114B (increment-core) (B). Aerial view of the Jamari National Forest site (C) tree positions for the* Cedrela fissilis *JAC09C and JAC21A, and* Peltogyne paniculata *JAR26C. Equator (black line) and the Dec/Jan/Feb-TLPB delimiting mean position (white dashed-line; adapted from Hua et al (2022)) is shown here for reference. Further details on wood samples characteristics are displayed in Figure 2.*

MTV001 shows some evidence of wedging rings (Figure 2), protocols were followed to select the sample materials for optimal ^{14}C results (i.e., laths that show rings with the earlywood and latewood boundaries clearly identified). The rationale of using both series, MTV001D and MTV114B, during the production of a complete post-1950 tree-ring ^{14}C record was associated with the compressed section near the bark of the MTV001 tree (Figure 2). While the compressed section did not pose a problem during dendrochronological dating, it did not allow for precise sampling of wood for ^{14}C analysis, as the rings in this section are far too narrow. Thus, we selected MTV114B series to complete the calendar years of the ^{14}C record (not shown in this work). We then arranged to overlap the two wood sample sequences for ^{14}C dating at the post-bomb slope section. This procedure assured us that high-quality data could be produced via several ^{14}C replicates. The 15 overlapping calendar years selected for ^{14}C analysis included duplicates of the single tree rings sampled from the cross-section MTV001D (the calendar years of 1964, 1966, and 1969), the increment core MTV114B (the calendar years of 1982, 1988, and 1989), and several others from both samples (nine calendar years between 1971 and 1980).

For the Jamari National Forest dendrochronology collections in the Southwestern Brazilian Amazon (red star in Figure 1A), three trees were selected for ^{14}C analysis (Figure 2B). Trees at this locality experience a hot, humid, and seasonally wet type of climate (precipitation occurs between October and May; Figure S1). Trees species of the dendrochronologically dated collections of *Peltogyne paniculata* and *Cedrela fissilis* were selected for our study (Santos et al. 2021 and Ortega-Rodriguez et al. 2023,
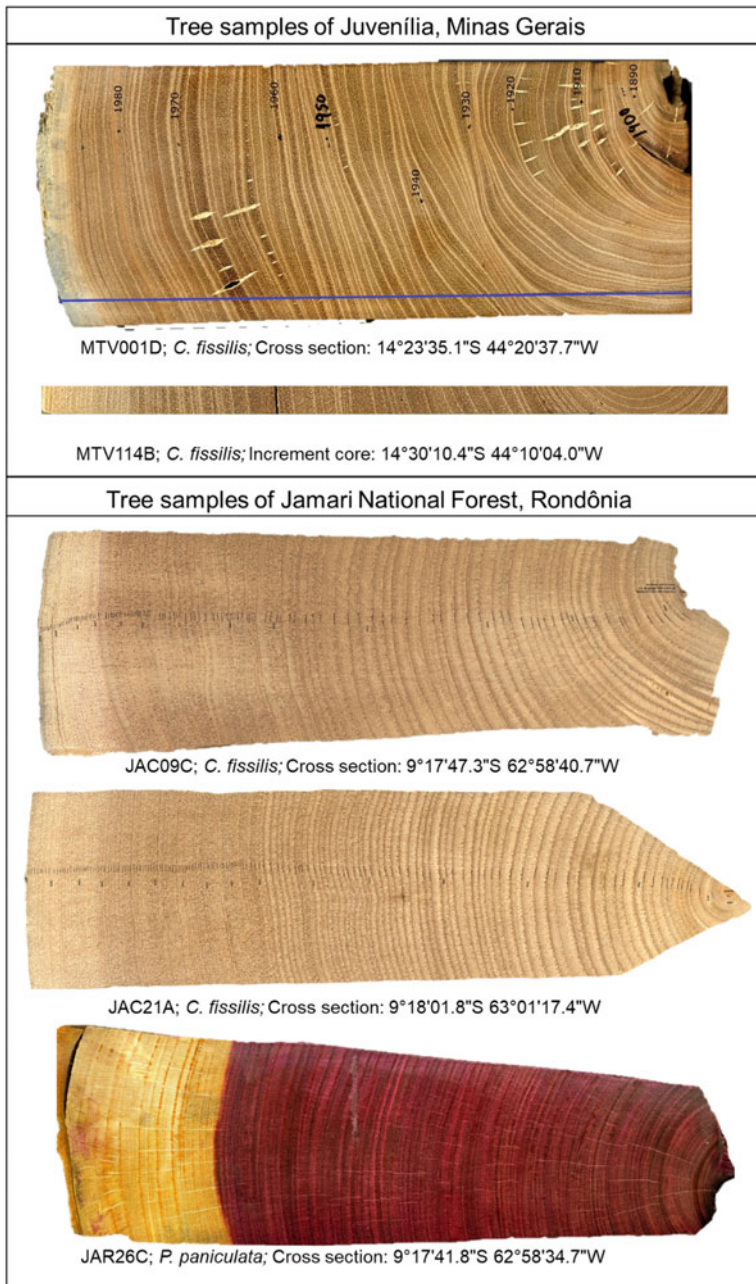
Figure 2. *Types of wood samples used in this study (A) from Juvenília, Minas Gerais, and (B) from Jamari National Forest, Rondônia dendrochronology field collections. Site coordinates, tree species, field deployable sampling method and sample identification are shown under each image. Examples of basic tree-ring sampling methods are shown in Figure S2, in supplementary material.*

respectively). Here, we took advantage of those two annually-resolved tree species within a mutual territory to test for equal $F^{14}C$ means (Figure 1C), assuming that if they are subjected to the same $^{14}CO_2$ air-masses they should have the same $F^{14}C$ value within error. In this case, we assume that *P. paniculata* tree species responses to the rainy season would be similar to those of *Cedrelas* at this location, even though their phenology has not been extensively examined yet.

From this site, 36 overlapping calendar years between 1955 and 1990 were tested. In all cases, at least two different trees were measured in replication, i.e., pairs/sets using same tree species (the *C. fissilis* cross-sections JAC09C and JAC21A, apart by at least 5 km), or different tree species (i.e., the *C. fissilis* cross-sections JAC09C and/or JAC21A, with the addition of a *P. paniculata* cross-section JAR26C located 0.2km from JAC09C, and ca. 5km from JAC21A).

The chronologies of both sites (BRA002 and BRA015) and the information of the tree-ring parameters of each sample can be accessed through the International Tree-Ring Data Bank (ITRDB, https://www.ncei.noaa.gov/products/paleoclimatology/tree-ring).

2.2 Sample handling for ^{14}C analysis

For satisfactory results, especially regarding tree ^{14}C reconstructions, dendrochronologically dated material sampled as single tree rings should contain the entire growing season. Thus, dendrochronology teams were advised to sample tree rings by cutting them along their delimited boundaries with great care without including neighboring rings. In Figure S3 (supplementary material) we illustrate suboptimal versus optimal tree-ring sampling for atmospheric ^{14}C reconstructions. Researchers can determine ring boundaries due to anatomical features of growth ring formation in tropical hardwoods, which can include density variation of fiber cells, marginal parenchyma bands, alternating parenchyma and fiber bands, vessel cluster frequencies and vessel diameter sizes (Worbes 1989, Quintilhan et al. 2021, Ortega-Rodriguez et al. 2022). Two recommendations were further advised: i) to facilitate the isolation of individual samples from cross-sections, we emphasized first cutting a thin radial cross-section from it (see examples in Santos et al. 2021, 2024; and Figure S3C); and ii) avoiding glue that is typically used to mount increment-cores for dendrochronology dating.

Once in the lab, before chemical extractions for ^{14}C dating analysis took place, individual tree-ring samples were meticulously inspected under a microscope to ensure that they were not overcut or undercut, or if they needed to be re-shaped (Figure 3). Earlywood and latewood fractions of tree rings can have different ^{14}C values (Haines et al. 2023; Kudsk et al. 2018). Thus earlywood/latewood fractions should also be carefully evaluated for their ability to represent a full growth-season. Enlarged images of each tree species' wood slabs or strips assisted in assessing the sampled tree-ring shapes. Undercut tree rings that potentially include a different year's carbon, or those of irregular earlywood to latewood shapes, may be adjusted by using a transversal cutting technique. Overcut tree rings that showed missing portions of the earlywood or latewood fractions were replaced by samples that could represent the entire annual growing season.

Here, all tree-ring samples were adequately evaluated for their quality regarding their earlywood and latewood fractions under the microscope. Later, they were weighed out for their total mass, then reduced to chips. Santos et al. (2023) favor wood chip reduction by cutting radial slivers of wood from the tree-ring chips above glazed ceramic dishes of different sizes, as it allows for easy wood fraction recovery without contamination (refer to video in the supplementary material of Santos et al. 2023). Once the wood was reduced to slivers, the samples were weighed out again. This procedure aimed for high recovery yields. On average, we obtained a wood recovery yield of 99.6% (n = 30 independent wood samples) for the Juvenília site, and 99.9% (n = 89 independent wood samples) for Jamari National Forest.

Chemical extractions to alpha-cellulose were performed on an aliquot of tree-ring slivers weighing 10–30 mg, following the protocol of Santos et al. (2023), which was adapted from a previous work of Southon and Magana (2010). The former chemical protocol produces pure alpha-cellulose extracts and well-mixed cellulose fibers. Chemical treatment can be summarized in the following steps. 1 N HCl and NaOH at 70°C cycling until the supernatant is clear. A bleaching step with 1 N HCl-NaClO$_2$ at 70°C was employed for about 6 hr. The alpha-cellulose residual fraction was reached after 17.5% NaOH treatment for 1–2 hr at room temperature. The alpha-cellulose fraction was then treated with 1 N HCl at 70°C to remove atmospheric CO$_2$ adsorbed during treatments and brought to a neutral pH. Cellulose fibers were homogenized in an ultra-sonic bath and dried for later processing.
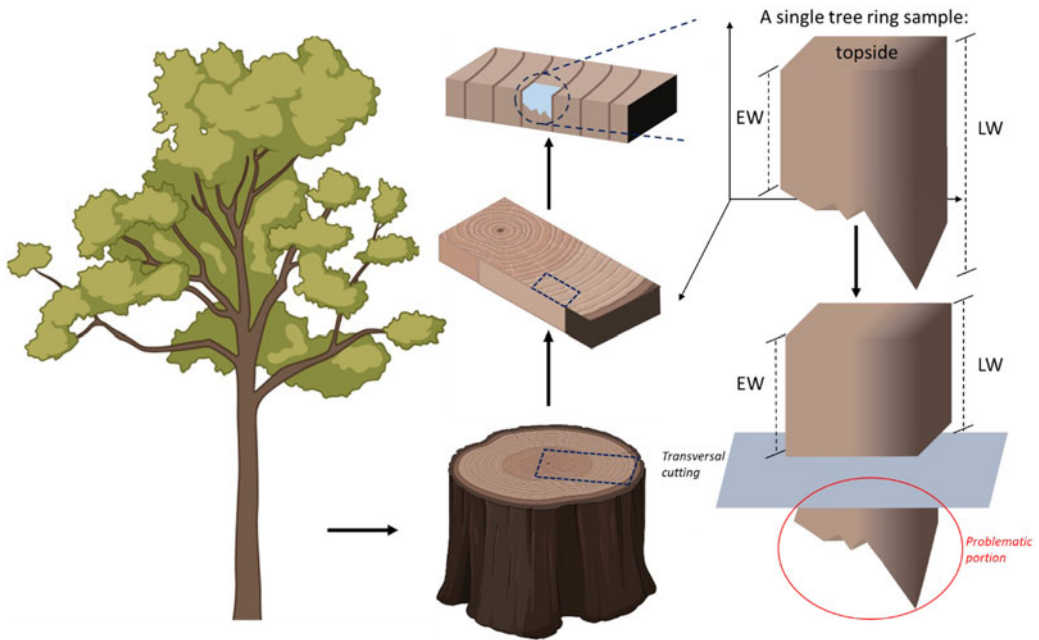
Figure 3. *Diagrammatic example of a misaligned tree ring received at the ^{14}C-AMS laboratory (top right). Uneven tree rings with earlywood (EW) light-colored band somewhat shorter, than the latewood (LW). ^{14}C-AMS laboratory and steps to trim the sample so the only potentially different dimension being sampled is the earlywood/latewood width. Proper transverse cutting will equalize the height and tangential dimensions of the ring block so only the ring widths would have different dimensions.*

For the purpose of ^{14}C-AMS measurements, alpha-cellulose extracts were loaded into pre-baked quartz tubes with CuO, sealed after evacuation, and burned at 900°C to produce CO_2. Later, CO_2 samples were released in a vacuum line, cryogenically cleaned and transferred to pre-baked vessels loaded with Zn/TiH_2 and Fe for the reduction of CO_2 to filamentous graphite (Santos and Xu et al. 2017). Graphite-Fe mixtures were pressed into target holders and underwent measurement by AMS, using an in-house modified NEC 0.5MV 1.5SDH-1 spectrometer equipped with online δ^{13}C-AMS capabilities (Beverly et al. 2010). This instrument typically allows for precision better than 0.3%, based on measurements of 6-7 targets of Oxalic acid I (OX-I or NIST HOxI SRM 4990B), as the primary standard. Combustible reference materials, such as OX-II (oxalic acid II) and ANU (sucrose), were used to confirm instrumentation precision levels. For quality control of alpha-cellulose chemical processing and for background, the reference materials of FIRI-J (barley mash) and AVR-07-PAL-37 (wood blank) were used, respectively. Radiocarbon measurements were performed on graphite targets of 0.4 to 0.9mgC. Those are considered regular-sized targets on our in-house modified NEC 0.5MV 1.5SDH-1 spectrometer, as no significant changes in beam current and/or uncertainties (precision) were observed. The data are reported as a fraction of modern carbon (F^{14}C), following the conventions shown in Stuiver and Polach (1977) and Reimer et al. (2004) when dealing with post-1950 AD samples.

3. Results and discussion

3.1 Assessment of ^{14}C results

To assess potential sources of error (such as, ^{14}C sample processing to graphite, measurement instrument bias errors, etc.) we measured combustible samples of OX-I, OX-II or ANU along with cellulose fibers. For alpha-cellulose analysis, we processed and measured duplicates of reference

materials, such as FIRI-J barley. In all instances, precision was on the order of 0.25% or lower. Precision fitness from tropical cellulose fibers was evaluated by the weighted mean $F^{14}C$ and propagated errors between ^{14}C results of pairs and/or sets of tree rings that shared the same calendar years of a given site. To assess alpha-cellulose homogeneity and tree-related variables influencing ^{14}C values, we compared ^{14}C results using several pair/set combinations. The legends in Figures 4 and 5 contain information about those combinations.

Data accuracy was appraised through the difference between the weighted mean $F^{14}C$ detected from tree rings for each site and the datasets associated with the Dec/Jan/Feb-TLPB-influenced regions, i.e., of SH1-2 or SH3 (Hua et al. 2022). Since atmospheric ^{14}C compilations still lack data in SH lower and middle latitudes, we posit that small ^{14}C differences are expected. For example, current SH1-2 and/or SH3 curves do not fully reflect latitudinal/longitudinal air mass circulation, terrestrial carbon isoflux effects, and/or local contributions of small nuclear tests after the 1963 Limited Test Ban Treaty around the world. In addition, Hua et al. (2022) assume that vegetation over SH grows during Dec/Jan/Feb, hence precise fine-tuning cannot be expected (see discussions in sections 3.1.1 and 3.1.2).

To visually compare data, we made use of a 2-dimensional scatter plot where dendrochronological dates (or calendar years AD) were directly compared to ^{14}C calibrated ages by CALIBomb software (http://calib.org/CALIBomb/). When corresponding dates from the two datasets were equal to each other, they fell exactly on the identity line 1:1 scatter plot. In order to convert the post-1950 AD $F^{14}C$ values obtained to ^{14}C calibrated ages, we first calculated the weighted mean of pairs/sets and their respective propagated and standard error. We used the greatest of two given errors of the weighted mean $F^{14}C$ values as inputs in CALIBomb to produce ≈95% (2-sigma errors; $P < 0.05$). As expected, when converting ^{14}C ages to ^{14}C calibrated ages after 1950 AD, each weighted mean $F^{14}C$ and error resulted in two possible ^{14}C calibrated age ranges. Thus, we selected the calibrated age ranges that were in closer proximity to the sequence of calendar ages expected for the dendrochronological dates.

To adjust the dendrochronological dates to the time when trees photosynthesized atmospheric $^{14}CO_2$ and form tree-ring cellulose, we made use of the length of the growing season at each site, which is associated with the rainy season (Figure S1). Even though annual variations in vegetation growth may occur, small differences from the growing-season length should not be sufficient to affect our conclusions. A decimal date was then centered in the middle of the growing season, while the length of the growth season was considered as the error-bar. Thus, for the Juvenília site all calendar dates were adjusted to 0.002 ± 0.166 (November to March; 4 months in total; Figure S1A), while for Jamari we used 0.042 ± 0.291 (October to May; 7 months in total; Figure S1B).

In the supplementary material, we also provide the $F^{14}C$ associated value of each calendar year's individual tree rings alongside the current atmospheric post-1950 AD ^{14}C calibration curves for each site (see Figures S4 and S5), as well as the ^{14}C data per dated tree (see Tables S2 and S3).

3.1.1 Juvenília samples ^{14}C data precision/accuracy performance

In Figure 4 we show the ^{14}C data precision/accuracy performance associated with the trees of the Juvenília site. A total of 15 replicate ^{14}C analyses were produced based on 30 measurements from this site.

In Figure 4A, we compared the data reproducibility based on propagated errors calculated for each weighted mean $F^{14}C$ result of the tree rings pairs. For the ^{14}C results/pairs that belong solely to the cross-section MTV001D and to the increment core MTV114B (cellulose homogeneity), and to those using both individual trees > 20km apart (Figure 1), we used the different symbols following the scheme shown in the figure 4A legend. Although our calculations are comparing just two data points per calendar year, the context and initial differences on how they were sampled, handled, and produced are enough to justify them. Here, 93% of replicated data (as cellulose fibers) yielded precision that is < 0.3% (n = 14 pairs/sets), while 67% are notably below 0.2% (n = 10 pairs/sets). Individual ^{14}C results are shown in Table S2 in the supplementary material. A standard pooled deviation, using all measured pairs, yielded 0.23% (n = 15 pairs).
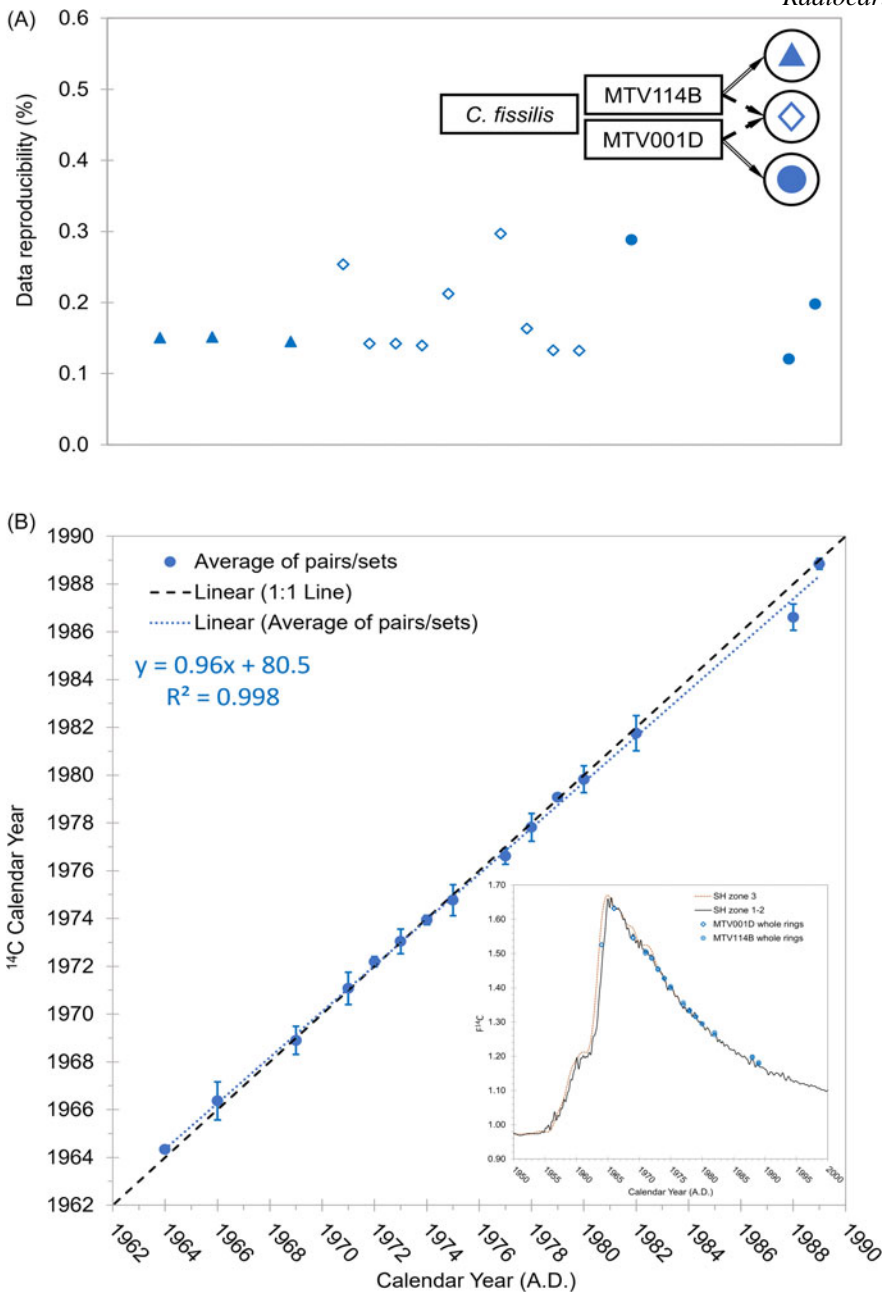
Figure 4. *Radiocarbon data performance associated with trees of the Juvenília site. (A) Data reproducibility among pairs for different tree samples for calendar years ranging between 1964 and 1989. The legend/diagram describes the combinations tested. Solid arrows represent pairs within a tree and dashed arrows between trees. (B) Dendrochronological assigned calendar years (x-axis) were adjusted to 0.002 (middle of the growing season, as described in text) versus ^{14}C-calibrated calendar years (y-axis) of averaged pairs/sets. The error for dendrochronological dates has been estimated based on the length of the growing season (i.e., ± 0.166; 4 months in total) and is hidden by symbols. The ^{14}C-calibrated calendar year errors were calculated based on age ranges derived by CALIBomb. The black-dashed line shows the 1:1 ratio that is expected if all ^{14}C-calibrated calendar years agree exactly with dendrochronological dates. Detailed results are provided in supplementary materials (Figure S4 and Table S2).*

Radiocarbon data accuracy was evaluated by using the description in section 3.1, and it is displayed in Figure 4B. Due to the location of the Juvenília site, outside of the TLPB boundary on South America (Figure 1A), we chose the SH1-2 curve (Hua et al. 2022) to estimate the ^{14}C calibrated ages based on the F^{14}C values derived from the tree rings. Note that the fragmented nature of the ^{14}C datasets in the SH1-2 led this compilation to be dominated by ^{14}C signatures from sites at higher southern latitudes in Australia and New Zealand. Nonetheless, besides the calendar year of 1988, our data in figure 4B show an excellent agreement with ^{14}C calibrated ages based on the SH1-2 curve (Hua et al. 2022) for all other Juvenília assigned calendar years (as homogenized alpha-cellulose fibers). The extremely high ^{14}C data consistency detected here on post-1950 *C. fissilis* tree-ring samples shows that field wood sample collection techniques (cross-sections versus increment core) as well as tree spatial distribution are not relevant for data heterogeneity overall (Figure 4B, dashed line = 1:1 match, solid line = best-fit linear regression, $R^2 = 0.998$).

3.1.2 Jamari National Forest samples ^{14}C data precision/accuracy performance

In Figure 5, we show the ^{14}C data precision/accuracy performance associated with the trees of the Jamari National Forest site. A total of 36 replications were performed based on 89 individual ^{14}C measurements.

Data reproducibility in Figure 5A represents the error associated with the weighted mean F^{14}C result of the tree-rings pairs/sets corresponding to each calendar year between 1955 and 1990. Reproducibility tests were more complex at this site, i.e., we explored possible differences between same individual trees/same species, pair/sets involving all tree species, and pairs/sets using two distinct tree species (legend in Figure 5A). The consistency of the ^{14}C data is rather similar among pairs/sets regardless of distances between trees (Figure 1), differences in tree species and/or pairs/sets combinations (Figure 2). Overall, most of the tree-ring calendar-year sets analyzed yielded a precision below 0.3% (83%), with the majority below 0.2% (64%). Reproducibility that fell between 0.3% and 0.8% (17%) are from pair/ sets that involved *P. paniculata* and one or both of the *C. fissilis* samples (Figure 5A).

Despite the noticeable differences in wood anatomy, density, and chemistry profiles between *P. paniculata* and *C. fissilis*, both species can produce climatically sensitive growth rings, well-defined by parenchyma bands (Ortega-Rodriguez et al. 2022). Thus, possible errors due to the delimitation of the ring boundaries can be completely ruled out. As recovery yield during laboratory wood chipping was close to 100%, problems regarding this step can also be ruled out. Third, we assumed that growth of *P. paniculata* and *C. fissilis* tree species in the Jamari National Forest occurred during similar time frames, as mentioned earlier. Still, maximum variance was observed just for pairs/sets related to the calendar years of 1962, 1963, and 1965, but not 1964 (Table S3). Throughout all those years, atmospheric ^{14}C changes during a single year were enormous, but that should include the 1964 calendar year as well. Thus, we suspect that small differences in tree life-cycles are not a major factor either. *P. paniculata,* also known as "purpleheart," has a higher wood density than *C. fissilis*, i.e., 0.80 versus 0.55 g/cm^3 (Zanne et al. 2009). In addition, the wood of *P. paniculata* has a straight or wavy grain (sometimes interlocked) and is loaded with resins (Galletly 1889). Those characteristics make wood working with *P. paniculata* more challenging, including sawing, planning, turning, drilling and shaping (ITTO, 2024; Wood Database). Thus, we suspect this was the main reason for the small variabilities (0.3% < x < 0.8%) observed for the ^{14}C pairs/sets of 1962, 1963 and 1965, but not to 1964. As mentioned before, isolation of whole single tree rings from denser and resinous woods by hand requires more skill, time and effort. Still, the ^{14}C results of multiple tree species, when combined as propagated error, did not exceed 0.8%. A pooled standard deviation yielded 0.35% by computing all measured pairs/sets (n = 36 pairs/sets). Given the difficulty of working with denser and/or resinous woods, our results are extremely encouraging. As annually-resolved rings in quantities for dendrochronology dating are not always available at key sites of interest in the tropics, overlapping tree species can be a viable option for ^{14}C reconstructions, when master chronologies are not feasible. However, sufficient ^{14}C data replication will be obviously required to assure data quality, as we demonstrated here.
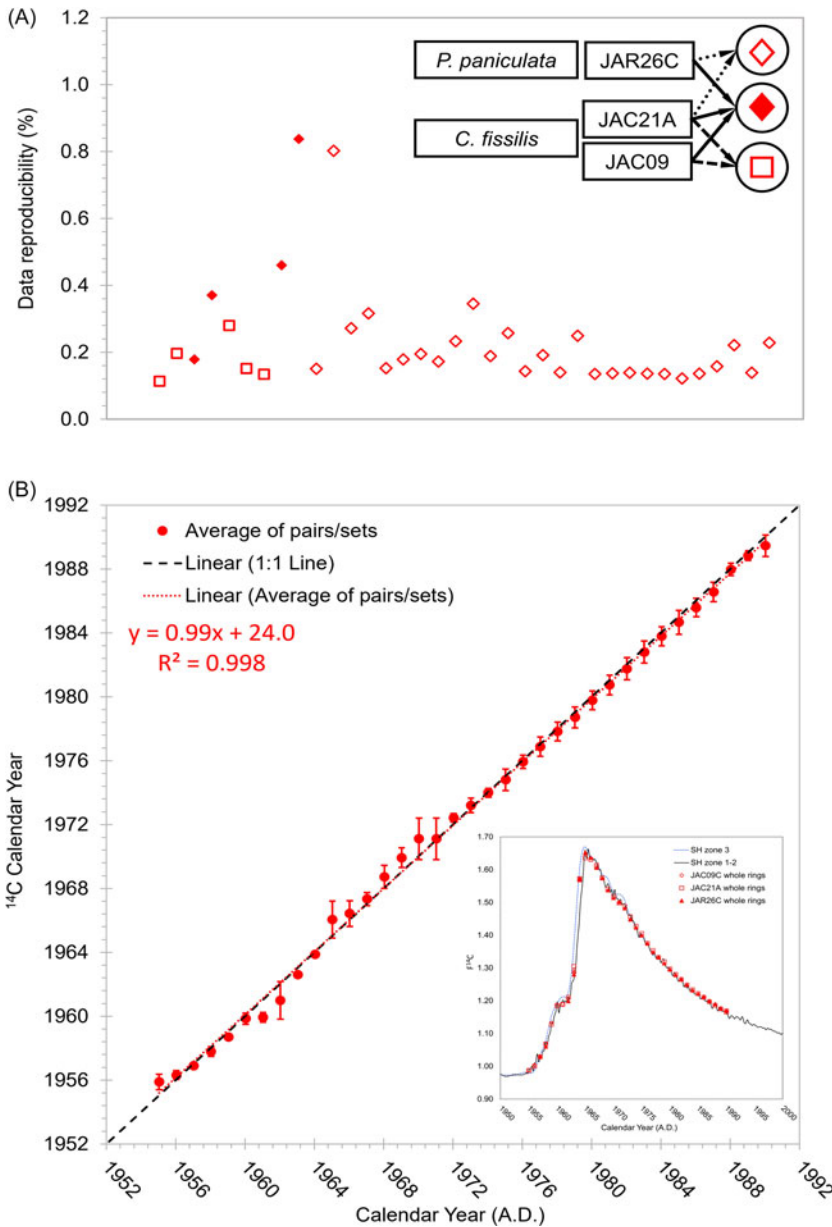
Figure 5. Radiocarbon data performance associated with the trees of the Jamari site. (A) Data reproducibility among sets of distinct tree samples of same or different tree species for calendar years between 1955 and 1990. The inset legend/diagram indicates the combinations tested. Open-square symbols compare reproducibility of two C. fissilis trees, open diamond symbols compare one C. fissilis *and one* P. paniculata *tree, and solid diamond symbols compare all three trees. (B) Dendrochronologically determined calendar years (x-axis) were adjusted to 0.042 (middle of the growing season, as described in text) versus ^{14}C calibrated calendar years (y-axis) of averaged pairs/sets. The error for dendrochronological dates has been estimated based on the length of the growing season (i.e., ± 0.291; 7 months in total), and are within the bounds of the symbol area. The ^{14}C calibrated calendar years errors were calculated based on age ranges derived by CALIBomb. The black-dashed line shows the 1:1 ratio that is expected if all ^{14}C calibrated calendar years agree exactly with dendrochronological dates. Detailed results are provided in supplementary materials (Figure S5 and Table S3).*

For this site, we also examined ^{14}C data accuracy by using the estimated ^{14}C calibrated ages averaging the F^{14}C values derived from the tree-rings pairs/sets and CALIBomb. Since Jamari National Forest seems to be inside the TLPB boundary in South America (Figure 1A), we chose SH3 curve to calibrate our data for this location (Hua et al. 2022). We observed that all Jamari National Forest assigned calendar years are in good (if not excellent) agreement with expected ^{14}C calibrated ages, regardless of the fact that 86% of these data make use of mixed tree species (Figure 5B, dashed line = 1:1 match, solid line = best-fit linear regression, R^2 =0.998). Here, slight differences in ^{14}C were mostly concentrated around the early 1960s and the 1970s. The first can be attributed to asymmetry among site longitudes and terrestrial carbon fluxes, as evidenced by Santos et al. (2024), when comparing ^{14}C records of the Eastern Amazon Basin, Brazil (1°S, 53°W; 1940–2016) and Muna Island (5°S, 122°E; 1951-1979; the backbone of the SH3 record—Hua et al. 2022). Regarding the 1970s, after the 1963 Limited Test Ban Treaty, we attribute differences in ^{14}C between our site and SH3 to China's Lop Nor nuclear tests (42.4°N, 88.3°E; 1964–1980). These nuclear tests have been detected in the Muna Island and the Huangzhong district, China (36.3°N, 101.7°E; Xiong et al 2021) ^{14}C records, but not at the Eastern Amazon Basin ^{14}C record (Santos et al. 2024). As the Jamari site is located in the Southwestern Brazilian Amazonia (Figure 1A), we suspect that this site would not capture Lop Nor nuclear tests as well (Figure S5). China's Lop Nor nuclear tests were about 2-5 Mt TNT in magnitude (Xiong et al 2021), and therefore would have a small influence in the upper atmosphere. Nonetheless, high consistency ^{14}C results obtained here on post-1950 tree-ring samples from distinct tree species (*P. paniculata* and *C. fissilis*) show that tree species diversity is not the primary factor influencing heterogeneity of results.

3.2 Relevance of findings

Physical and chemical tree-ring preparation are essential prerequisites for precise and accurate results during ^{14}C analysis. However, the many involved steps during sample handling and processing can add unwanted errors. Santos et al. (2023) laid out steps on how to prevent and reduce errors when analyzing single trees for atmospheric ^{14}C reconstructions and applied those techniques to produce tropical tree-ring ^{14}C records using parenchyma-rich *Hymenolobium petraeum* and *Cedrela odorata* tree species from the Amazon Basin (Santos et al. 2023 and 2024, respectively). However, questions remained regarding other tropical tree species and the possibility of combining several trees or tree species from a given region to derive fine-tuned atmospheric ^{14}C information.

Here, we tested a number of *Cedrela fissilis* samples (i.e., multiple trees) from two sites in South America, from dry and wet forests. Trees from each dendrochronological collection were separated by 5 or 22.5 km and were from cross-sections or increment cores. Our ^{14}C results also represent samples from species with distinctly different wood density, i.e., *C. fissilis* (0.55 g/cm^3) and *P. paniculata* (0.80 g/cm^3) (Zanne et al. 2009). In sum, 15 pairs of ^{14}C results from the Juvenília site and another 36 from the Jamari site, which include multiple tree species combinations are shown. In all instances, ^{14}C data appear precise and accurate within error, and therefore external factors (such as microhabitat-related conditions affecting trees) do not appear to be relevant for bomb-induced ^{14}C variability in the tropics.

Precision frequency distributions are shown in Figure 6 for the pair/sets presented in this study and those of duplicated tree ^{14}C data using *Araucaria aungustifolia* (n = 9 pairs; Santos et al. 2015), *Pinus radiata* and *Agathis australis* (n = 14 pairs; Turnbull et al. 2017), and *Polylepis tarapacana* (n = 21 pairs; Ancapichún et al. 2021) that have been included in the global post-1950 map with replicated data (Hua et al. 2022). Except for the later work (i.e., Ancapichún et al. 2021, which used more than one tree of the same species in their replication analysis), the former two studies reported ^{14}C results of pairs of the same trees. Note that we chose not to add the Campbell Island tree ^{14}C record of Turney et al. (2018) in this evaluation. Due to low tree availability across this region, this record was constructed with multiple distinct single trees that bear large calendar date errors. Thus, some inherent variability in the Campbell Island tree ^{14}C record is expected.
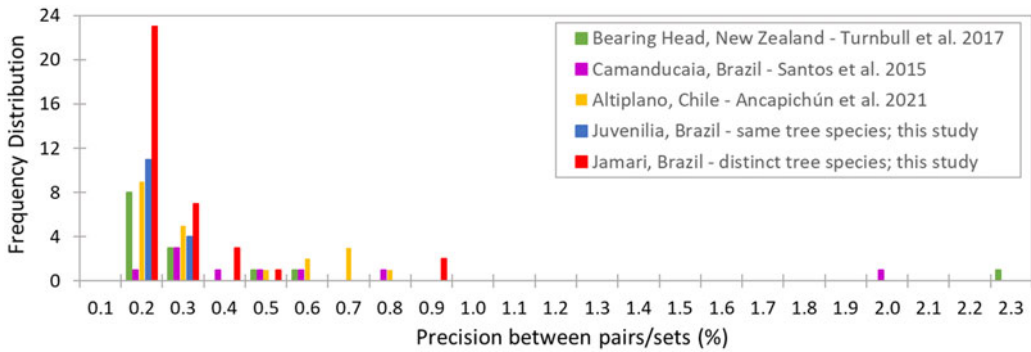
Figure 6. *Frequency distribution versus* ^{14}C *precision of pair/sets from several sites and studies. Number of replicated pairs/sets were variable, i.e., 14 pairs from Bearing Head (Turnbull et al. 2017), 9 pairs from Camanducaia (Santos et al. 2015), 21 pairs from Altiplano (Ancapichún et al. 2021), and 51 pairs/sets from this study (15 pairs from Juvenília and 36 from Jamari sites). Precision bins are shown as percentages (%).*

Poor performance in tree ^{14}C data is sometimes attributed to chemical procedures adopted by laboratories, earlywood nonstructural carbon transfer or other confounding factors that are difficult to demonstrate. Here, we evaluate tree ^{14}C data fitness using a wider range of factors, including dry and wet forests, individual tree distances, and distinct tree species together with wood's variable properties (density). Regardless of the combinations assessed (Figures 4 and 5), our data show a large proportion of ^{14}C results with minimum variance (close to 0.3% or lower). This outcome is similar or even better than that of other studies (Figure 6). We can conclude that careful wood and cellulose processing (prior ^{14}C measurements) played important roles in precision of data.

The findings reported here are significant, as by improving ^{14}C data consistency among several trees/ sites, researchers can fill several spatial and temporal gaps and/or improve atmospheric ^{14}C data in a more comprehensive manner. Moreover, even though the Amazon Basin hosts over 16,000 tree species (Ter Steege et al. 2015), not all those tree species show annual growth rings. Plus, those that show annual growth may not occur within the same micro-environment or may not be long-living species (Linares et al. 2017). Thus, combining tree species for a given site to derive atmospheric ^{14}C information may be required. Here, we demonstrated that this is feasible when we overlapped *C. fissilis* and *P. Paniculata* tree species. In addition, mapping present-day $^{14}CO_2$ distribution in trees in places where air-sampling stations are mostly scarce (such as the tropics) is relevant to better evaluating future changes, e.g., how atmospheric circulation may change as the climate warms (TLPB expansion or displacement), and how trees will cope under extreme climate conditions (physiological responses). While our efforts to improve ^{14}C data quality focus on tropical trees in general during the post-1950 AD period, we believe that the steps adopted here can also be used on extratropical tree species, other ^{14}C age-ranges, and applications.

Achieving robust ^{14}C data consistency can be then attributed to the coordinated procedures of careful handling of whole tree rings during physical individual sampling from wood laths and laboratory steps, a straightforward chemical extraction procedure (Santos et al. 2023, Griffin et al. 2024), as well as homogenization of cellulose once chemical extractions reach completion. The latter is useful when cellulose extracts per individual tree ring are significantly large, as just a fraction of it will be used for further ^{14}C sample processing.

4. Conclusions and further recommendations

A fundamental limitation to any scientific question is normally associated with the overall data uncertainty. In tree-ring ^{14}C analysis, which involves considerable sample handling and processing, data

uncertainty can sometimes become overwhelming. Hence, important questions can no longer be answered. While the overall data uncertainty can never be reduced to zero due to analytical errors inherent in ^{14}C-AMS measurements, the implementation of careful methodologies while handling tree-ring samples can help reduce sample processing errors.

In this work, we reported post-1950 AD ^{14}C replicated results from tropical tree rings sampled from dendrochronological collections containing *Peltogyne paniculata* and multiple *Cedrela fissilis* tree species. The tree rings tested showed different anatomical and chemical characteristics and were collected from two separate sites on South America under different precipitation regimes. Moreover, replicated data involved trees spaced apart by significant distances and/or combined different tree species. Regardless of the criteria differences among distinctive types of trees/sites tested, variance and accuracy among ^{14}C results were fully reproducible. Thus, the most important criteria for ^{14}C data consistency were credited to careful tree-ring sampling and handling at both laboratories (tree ring and ^{14}C), followed by thorough homogenization of cellulose fibers before ^{14}C sample processing and analysis took place. By following those strategies, whole rings representing the intake ^{14}C for a full growing season were properly detected and reproduced within uncertainties.

For most cases, the sum of all variances in the final tree-ring ^{14}C measurements were 0.3% or lower (88% of the data) regardless of the distances between trees, especially when the same tree species with similar density levels were used. The overall high-performance for our post-1950 AD results, which involved a comprehensive number of tree-ring ^{14}C measurements (n = 119 individual measurements in total), allowed us to obtain a more accurate picture of the ^{14}C concentration of those tree rings. Our results suggest that several trees from the tropics with continuous annual growth patterns that can be discerned by dendrochronology methods, can also be incorporated into fine-tuned atmospheric ^{14}C reconstructions, when variance-reduction strategies (as those reported here) are applied. Further recommendations for future ^{14}C datasets would include sufficient data replication per ^{14}C records produced, for a better understanding of data and the factors affecting them.

References

Ancapichún S, De Pol-Holz R, Christie DA, Santos GM, Collado-Fabbri S, Garreaud R, Lambert F, Orfanoz-Cheuquelaf A, Rojas M, Southon J and Turnbull JC (2021) Radiocarbon bomb-peak signal in tree-rings from the tropical Andes register low latitude atmospheric dynamics in the Southern Hemisphere. *Science of the Total Environment* **774**, 145126. https://doi.org/10.1016/j.scitotenv.2021.145126.

Baker JC, Santos GM, Gloor M and Brienen RJ (2017) Does Cedrela always form annual rings? Testing ring periodicity across South America using radiocarbon dating. *Trees* **31**, 1999–2009. https://doi.org/10.1007/s00468-017-1604-9.

Beverly RK, Beaumont W, Tauz D, Ormsby KM, von Reden KF, Santos GM and Southon JR (2010) The Keck carbon cycle AMS laboratory, University of California, Irvine: status report. *Radiocarbon* **52**(2), 301–309. https://doi.org/10.1017/S0033822200045343.

Brienen RJW, Schöngart J and Zuidema PA (2016) Tree rings in the tropics: insights into the ecology and climate sensitivity of tropical trees. In Goldstein G and Santiago LS (eds). *Tropical Tree Physiology: Adaptations and Responses in a Changing Environment*. Springer International Publishing, 439–461. https://doi.org/10.1007/978-3-319-27422-5_20.

Bronk Ramsey C (2023) Radiocarbon calibration: from bane to blessing. *Radiocarbon*. https://doi.org/10.1017/RDC.2023.32.

Capano M, Miramont C, Guibal F, Kromer B, Tuna T, Fagault Y and Bard E (2018) Wood ^{14}C dating with AixMICADAS: Methods and application to tree-ring sequences from the Younger Dryas event in the southern French Alps. *Radiocarbon* **60**(1), 51–74.

Cercatillo S, Friedrich M, Kromer B, Paleček D and Talamo S (2021) Exploring different methods of cellulose extraction for ^{14}C dating. *New Journal of Chemistry* **45**(20), 8936–8941. https://doi.org/10.1039/D1NJ00290B.

Cohen J (1988) *Statistical Power Analysis for the Behavioral Sciences*, 2nd edition. Hillsdal: Lawrence Erlbaum, 1–579. ISBN: 978-0805802832.

Enting IG (1982) *Nuclear Weapons Data for Use in Carbon Cycle Modelling*. Commonwealth Scientific and Industrial Research Organization, Australia, 1–19.

Fogtmann-Schulz A, Kudsk SG, Adolphi F, Karoff C, Knudsen MF, Loader NJ, Muscheler R, Trant PL, Østbø SM and Olsen J (2021) Batch processing of tree-ring samples for radiocarbon analysis. *Radiocarbon* **63**(1), 77–89.

Fontana C, López L, Santos GM, Villalba R, Hornink B, Assis-Pereira G, Roig FA and Tomazello-Filho M (2024) A new chronology of Cedrela fissilis (Meliaceae) for Southern Brazil: Combining classical dendrochronology and radiocarbon dating. *Dendrochronologia* **85**, 126214. doi: 10.1016/j.dendro.2024.126214.

Galletly A (1889) Observations on the wood of certain resin-producing trees. *Part II. Transactions of the Botanical Society of Edinburgh* **17**(1–4), 381–388.

Gaudinski JB, Dawson TE, Quideau S, Schuur EA, Roden JS, Trumbore SE, Sandquist DR, Oh SW and Wasylishen RE (2005) Comparative analysis of cellulose preparation techniques for use with ^{13}C, ^{14}C, and ^{18}O isotopic measurements. *Analytical Chemistry* **77**(22), 7212–7224.

Griffin JN, Santos GM, Nguyen LD, Rodriguez DR, Pereira LG, Jaén-Barrios N, Assis-Pereira G, de Oliveira Barreto N, Brandes AF, Barbosa AC and Groenendijk P (2024) Demystifying the tropics: FTIR characterization of pantropical woods and their α-cellulose extracts for past atmospheric ^{14}C reconstructions. *Science of the Total Environment* **949**, 175010. https://doi.org/10.1016/j.scitotenv.2024.175010.

Hadad MA, Santos GM, Junent FAR and Grainger CS (2015) Annual nature of the growth rings of Araucaria araucana confirmed by radiocarbon analysis. *Quaternary Geochronology* **30**, 42–47. https://doi.org/10.1016/j.quageo.2015.05.002.

Haines HA, Hiscock WT, Palmer JG, Turney CS, Thomas ZA, Cadd H, Vohra J and Marjo CE (2023) The accuracy and precision of small-sized modern wood samples analyzed at the Chronos 14CARBON-CYCLE Facility. *Radiocarbon* **65**(2), 561–571. https://doi.org/10.1017/RDC.2023.4.

Haines HA, Olley JM, English NB and Hua Q (2018) Anomalous ring identification in two Australian subtropical Araucariaceae species permits annual ring dating and growth-climate relationship development. *Dendrochronologia* **49**, 16–28. https://doi.org/10.1016/j.dendro.2018.02.008.

Hua Q, Turnbull JC, Santos GM, Rakowski AZ, Ancapichún S, De Pol-Holz R, Hammer S, Lehman SJ, Levin I, Miller JB and Palmer JG (2022) Atmospheric radiocarbon for the period 1950-2019. *Radiocarbon* **64**(4), 723–745. https://doi.org/10.1017/RDC.2021.95.

ITTO (2024) Tropical Timber Database. Available at: http://www.tropicaltimber.info/es/specie/amarante-peltogyne-paniculata/#lower-content (Accessed: 5 February 2024).

Kudsk SG, Olsen J, Hodgins GW, Molnár M, Lange TE, Nordby JA, Jull AT, Varga T, Karoff C and Knudsen MF (2021) An intercomparison project on ^{14}C from single-year tree rings. *Radiocarbon* **63**(5), 1445–1452. https://doi.org/10.1017/RDC.2018.97.

Kudsk SG, Olsen J, Nielsen LN, Fogtmann-Schulz A, Knudsen MF and Karoff C (2018) What is the carbon origin of early-wood? *Radiocarbon* **60**(5), 1457–1464.

Levin I and Hesshaimer V (2000) Radiocarbon—a unique tracer of global carbon cycle dynamics. *Radiocarbon* **42**, 69–80. https://doi.org/10.1017/S0033822200053066.

Linares R, Santos HC, Brandes AFN, Barros CF, Lisi CS, Balieiro FC and de Faria SM (2017) Exploring the ^{14}C bomb peak with tree rings of tropical species from the Amazon forest. *Radiocarbon* **59**(2), 303–313. https://doi.org/10.1017/RDC.2017.10.

Michczyńska DJ, Krąpiec M, Michczyński A, Pawlyta J, Goslar T, Nawrocka N, Piotrowska N, Szychowska-Krąpiec E, Waliszewska B and Zborowska M (2018) Different pretreatment methods for ^{14}C dating of Younger Dryas and Allerød pine wood (*Pinus sylvestris* L.). *Quaternary Geochronology* **48**, 38–44. https://doi.org/10.1016/j.quageo.2018.07.013.

Němec M, Wacker L, Hajdas I and Gäggeler H (2010) Alternative methods for cellulose preparation for AMS measurement. *Radiocarbon* **52**(3), 1358–1370.

Novello VF, Cruz FW, Vuille M, Stríkis NM, Edwards RL, Cheng H, Emerick S, De Paula MS, Li X, Barreto ED and Karmann I (2017) A high-resolution history of the South American Monsoon from Last Glacial Maximum to the Holocene. *Scientific Reports* **7**(1), 44267. https://doi.org/10.1038/srep44267.

Ortega-Rodriguez DR, Hevia A, Sánchez-Salguero R, Santini L, de Carvalho HWP, Roig FA and Tomazello-Filho M (2022) Exploring wood anatomy, density and chemistry profiles to understand the tree-ring formation in Amazonian tree species. *Dendrochronologia* **71**, 125915. https://doi.org/10.1016/j.dendro.2021.125915.

Ortega-Rodriguez DR, Sánchez-Salguero R, Hevia A, Granato-Souza D, Cintra BB, Hornink B, Andreu-Hayles L, Assis-Pereira G, Roig FA and Tomazello-Filho M (2023) Climate variability of the southern Amazon inferred by a multi-proxy tree-ring approach using Cedrela fissilis Vell. *Science of the Total Environment* **871**, 162064. https://doi.org/10.1016/j.scitotenv.2023.162064.

Pearson S, Hua Q, Allen K and Bowman DM (2011) Validating putatively cross-dated Callitris tree-ring chronologies using bomb-pulse radiocarbon analysis. *Australian Journal of Botany* **59**(1), 7–17. https://doi.org/10.1071/BT10164.

Pereira GDA, Barbosa ACMC, Torbenson MCA, Stahle DW, Granato-Souza D, Santos RMD and Barbosa JPD (2018) The climate response of Cedrela fissilis annual ring width in the Rio São Francisco basin, Brazil. *Tree-Ring Research* **74**(2), 162–171. https://doi.org/10.3959/1536-1098-74.2.162.

Quintilhan MT, Santini Jr L, Rodriguez DRO, Guillemot J, Cesilio GHM, Chambi-Legoas R, Nouvellon Y and Tomazello-Filho M (2021) Growth-ring boundaries of tropical tree species: Aiding delimitation by long histological sections and wood density profiles. *Dendrochronologia* **69**, 125878. https://doi.org/10.1016/j.dendro.2021.125878.

Reimer PJ, Austin WE, Bard E, Bayliss A, Blackwell PG, Ramsey CB, Butzin M, Cheng H, Edwards RL, Friedrich M and Grootes PM (2020) The IntCal20 Northern Hemisphere radiocarbon age calibration curve (0–55 cal kBP). *Radiocarbon* **62**(4), 725–757. https://doi.org/10.1017/RDC.2020.41.

Reimer PJ, Brown TA and Reimer RW (2004) Discussion: Reporting and calibration of post bomb ^{14}C data. *Radiocarbon* **46**, 1299–1304. https://doi.org/10.1017/S0033822200033154.

Santos GM, Albuquerque RP, Barros CF, Ancapichún S, Oelkers R, Andreu-Hayles L, De Faria SM, De Pol-Holz R and das Neves Brandes AF (2022) High-precision ^{14}C measurements of parenchyma-rich Hymenolobium petraeum tree species confirm bomb-peak atmospheric levels and reveal local fossil-fuel CO_2 emissions in the Central Amazon. *Environmental Research* **214**, 113994.

Santos GM, Granato-Souza D, Ancapichún S, Oelkers R, Haines HA, De Pol-Holz R, Andreu-Hayles L, Hua Q and Barbosa AC (2024) A novel post-1950 CE atmospheric ^{14}C record for the tropics using absolutely dated tree rings in the equatorial Amazon. *Science of The Total Environment* **918**, 170686. https://doi.org/10.1016/j.scitotenv.2024.170686.

Santos GM, Granato-Souza D, Barbosa AC, Oelkers R and Andreu-Hayles L (2020) Radiocarbon analysis confirms annual periodicity in Cedrela odorata tree rings from the equatorial Amazon. *Quaternary Geochronology* **58**, 101079.

Santos GM, Komatsu AS, Renteria Jr JM, Brandes AF, Leong CA, Collado-Fabbri S and De Pol-Holz R (2023) A universal approach to alpha-cellulose extraction for radiocarbon analysis of ^{14}C-free to post-bomb ages. *Quaternary Geochronology* **74**, 101414.

Santos GM, Linares R, Lisi CS and Tomazello Filho M (2015) Annual growth rings in a sample of Paraná pine (Araucaria angustifolia): Toward improving the ^{14}C calibration curve for the Southern Hemisphere. *Quaternary Geochronology* **25**, 96–103.

Santos GM, Rodriguez DRO, Barreto NDO, Assis-Pereira G, Barbosa AC, Roig FA and Tomazello-Filho M (2021) Growth assessment of native tree species from the southwestern Brazilian Amazonia by post-AD 1950 ^{14}C analysis: Implications for tropical dendroclimatology studies and atmospheric ^{14}C reconstructions. *Forests* **12**(9), 1177. https://doi.org/10.3390/f12091177.

Santos GM and Xu X (2017) Bag of tricks: a set of techniques and other resources to help ^{14}C laboratory setup, sample processing, and beyond. *Radiocarbon* **59**(3), 785–801. https://doi.org/10.1017/RDC.2016.43.

Sookdeo A, Kromer B, Büntgen U, Friedrich M, Friedrich R, Helle G, Pauly M, Nievergelt D, Reinig F, Treydte K and Synal HA (2020) Quality dating: a well-defined protocol implemented at ETH for high-precision ^{14}C-dates tested on late glacial wood. *Radiocarbon* **62**(4), 891–899. https://doi:10.1017/RDC.2019.132.

Southon JR and Magana AL (2010) A comparison of cellulose extraction and ABA pretreatment methods for AMS ^{14}C dating of ancient wood. *Radiocarbon* **52**(3), 1371–1379. https://doi.org/10.1017/S0033822200046452.

Stuiver M and Polach HA (1977) Discussion: Reporting of [14]C Data. *Radiocarbon* **19**, 355–363. https://doi.org/10.1017/S0033822200003672.

Svarva H, Grootes P, Seiler M, Stene S, Thun T, Værnes E and Nadeau MJ (2019) The 1953–1965 rise in atmospheric bomb ^{14}C in central Norway. *Radiocarbon* **61**(6), 1765–1774. https://doi.org/10.1017/RDC.2019.98.

Ter Steege H, Pitman NC, Killeen TJ, Laurance WF, Peres CA, Guevara JE, Salomão RP, Castilho CV, Amaral IL, de Almeida Matos FD and de Souza Coelho L (2015) Estimating the global conservation status of more than 15,000 Amazonian tree species. *Science Advances* **1**(10), e1500936. https://doi.org/10.1126/sciadv.1500936.

Turnbull JC, Mikaloff Fletcher SE, Brailsford GW, Moss RC, Norris MW and Steinkamp K (2017) Sixty years of radiocarbon dioxide measurements at Wellington, New Zealand: 1954–2014. *Atmospheric Chemistry and Physics* **17**(23), 14771–14784. https://doi.org/10.5194/acp-17-14771-2017.

Turney CSM, Palmer J, Maslin M, Hogg A, Fogwill CJ, Southon J, Fenwick P, Helle G, Wilmshurst J, McGlone M, Bronk Ramsey C, Thomas Z, Lipson M, Beaven B, Jones RT, Andrews O and Hua Q (2018) Global peak in atmospheric radiocarbon defines the onset of Anthropocene Epoch in 1965. *Scientific Reports* **8**, 3293. https://doi.org/10.1038/s41598-018-20970-5.

Wood Database (2024) Purpleheart. Available at: https://www.wood-database.com/purpleheart/ (Accessed: 28 February 2024).

Worbes M (1989) Growth rings, increment and age of trees in inundation forests, savannas and a mountain forest in the neotropics. *IAWA Bulletin* **10**(2), 109–122.

Xiong X, Zhou W, Hou X, Cheng P, Du H, Zhao X, Wu S, Hou Y, Lu X and Fu Y (2021) Time series of atmospheric $\Delta^{14}CO_2$ recorded in tree rings from Northwest China (1957–2015). *Chemosphere* **272**, 129921.

Zanne AE, Lopez-Gonzalez G, Coomes DA, Ilic J, Jansen S, Lewis SL, Miller RB, Swenson NG, Wiemann MC and Chave J (2009) Global wood density database. Dryad. Available at: http://hdl.handle.net/10255/dryad.235.